ATMOSPHERIC SCIENCE LETTERS
Atmos. Sci. Let. **11**: 46–50 (2010)
Published online 1 February 2010 in Wiley InterScience
(www.interscience.wiley.com) **DOI:** 10.1002/asl.255

RMetS
Royal Meteorological Society

What causes the extremely heavy rainfall in Taiwan during Typhoon Morakot (2009)?

Xuyang Ge,[1]* Tim Li,[1] Shengjun Zhang,[1,2] and Melinda Peng[3]
[1] *International Pacific Research Center, SOEST, University of Hawaii, Honolulu, HI, USA*
[2] *State Key Laboratory of Severe Weather, Chinese Academy of Meteorological Sciences, Beijing, China*
[3] *Marine Meteorology Division, Naval Research Laboratory, Monterey, CA, USA*

**Correspondence to:*
Dr Xuyang Ge, University of Hawaii, 1680 East-West Road, POST Building 401, Honolulu, Hawaii 96822, USA.
E-mail: xuyang@hawaii.edu

Received: 22 September 2009
Revised: 29 November 2009
Accepted: 2 December 2009

Abstract

Despite its category-2 intensity only, Typhoon (tropical cyclone in the Western Pacific) Morakot produced a record-breaking rainfall in Taiwan. A cloud-resolving model is used to simulate this extreme rainfall event and understand the dynamic aspect under this event. Due to the interaction between Morakot and a monsoon system, a peripheral gale force monsoon surge appears to the south of Taiwan. The monsoon surge remains even in a sensitivity experiment in which Taiwan terrain is reduced. However, the rainfall amount in Taiwan is greatly reduced without high topography over Taiwan, suggesting the important role the local topography plays in producing heavy rainfall. The overall numerical results indicate that it is the interaction among the typhoon, monsoon system, and local terrain that led to this extreme event. Copyright © 2010 Royal Meteorological Society

Keywords: heavy rainfall; typhoon

1. Introduction

Tropical cyclones (TCs) make direct threats through its destructive winds and heavy rainfall to human lives and properties along the coast. Recently, Typhoon Morakot (2009) led to the worst flooding in the last 50 years in Taiwan. The storm produced an accumulated rainfall of 2777 mm during this event, surpassing the previous record of 1736 mm set by Typhoon Herb (1996). The extreme amount of rain within such a short period triggered enormous mudslides and severe flooding throughout Southern Taiwan. It wrought catastrophic damage, leaving nearly 700 deaths and roughly $4.7 billion USD in damages. Efforts have been made to understand the processes responsible for the heavy rainfall. In general, TC rainfall distribution depends on the internal structure of the TC. For example, the size of the eyewall determines, to the first order, the location of the maximum rain rate (Lonfat *et al.*, 2004). Other factors include TC interactions with the topography and large-scale monsoon circulation. The Central Mountain Range (CMR) in Taiwan with an average height of about 3 km may greatly modify TC tracks (Yeh and Elsberry, 1993) and impact the rainfall distribution (Wu and Kuo, 1999; Peng and Chang, 2002). Interactions between a TC and a large-scale monsoon circulation may also lead to a rainfall pattern that deviates substantially from TC rainfall climatology (Wu *et al.*, 2009). As will be discussed later, Typhoon Morakot was originated from a monsoon gyre characterized by a huge (with a half wavelength in the order of 3000 km) low-level cyclonic vortex. This type of gyre systems usually persists for 2–4 weeks and occurs roughly once in a year (Lander, 1994). It may have a great impact on TC genesis and subsequent motion. Morakot (2009) is chosen as an example to study the complex interactions among the TC, monsoon gyre, and terrain.

This article is organized as in the following: the numerical model and experiment designs are described in Section 2. In Section 3, results from the control experiment and a sensitivity experiment that reduces the topography over Taiwan are presented and the possible mechanism responsible for the extremely heavy rainfall and sudden TC track change is discussed. Finally, a summary and discussions are given in Section 4.

2. Model and experiment designs

The Advanced Research Weather Research and Forecasting model (WRF-ARW) is used for this study. Three nested domains with horizontal resolution of 27, 9, and 3 km are used. The outer and middle domains have 201 × 201 and 301 × 301 grid points, covering the regions (3–45 °N, 100–150 °E) and (12–37 °N, 110–138 °E), respectively. The inner finest resolution domain that has 181 × 181 grid points is moving with the storm. There are 27 levels in the vertical. The Kain–Fritch convective scheme (Kain and Fritch, 1993) is applied to the outer coarse mesh, and the convection is resolved explicitly in the middle and inner meshes. WSM 5-class microphysics scheme (Hong *et al.*, 2004) and the Yonsei University PBL scheme (Noh *et al.*, 2003) are used. Both longwave and shortwave radiation calculations are included in the simulations. The model simulation is integrated from 1200 UTC 5 August to 0000 UTC 10 August 2009.

The global analyses from the National Centers for Environmental Prediction (NCEP) final analyses (FNL) with 1° × 1° latitude–longitude resolution are used to initialize the model. However, the low resolution of the FNL analyses cannot resolve the structure of Morakot adequately, which will affect its evolution. Therefore, a TC initialization scheme, identified as the TC dynamic initialization (TCDI) package, is used for the model initial fields for better representation of Morakot's structure. The TCDI package includes two major components. The first part is the removal of the TC vortex in the initial field. The original vortex in the FNL analyses is removed and the environmental field is retained using the filtering technique developed by Kurihara *et al*. (1995). The second part is a dynamic initialization of a TC vortex spun up with a full nonlinear dynamics and physics in a quiescent environment. During the spin-up period, an initial Rankine vortex with a radius of maximum wind (R_{max}) 100 km and size of 1000 km (where vortex wind speed becomes zero) is forced toward the observed central minimum sea level pressure (MSLP). The final TCDI result is a balanced TC vortex with the MSLP of 970 hPa as observed. This dynamic- and thermodynamic-balanced TC vortex is then added back to the environmental field at the best track position issued by Japan Meteorological Agency (JMA).

Two numerical experiments are carried out. In the control run (CTL), the realistic Taiwan topography is used in the model. To examine the topographic effect, we conduct a sensitivity experiment (TOP100), in which the topography over Taiwan Island is set to be 100 m if the elevation is higher than this value. Through the comparisons between the two experiments, we investigate the possible roles of Taiwan orography and the monsoon gyre–TC interaction in causing this extreme rainfall event.

3. Results

Morakot formed in a large monsoon gyre over the Western North Pacific (WNP) on 2 August 2009. The TC gradually intensified as it tracked westward toward Taiwan. Due to the relatively large size of the typhoon, the barometric pressure steadily decreased, whereas the maximum wind increased slightly. Morakot weakened slightly while it made landfall in central Taiwan on later 7 August. Figure 1 compares the simulated and observed TC intensities and tracks from JMA best track data. Regarding the slow movement speed and landfall point, the CTL matches the observation reasonably well (Figure 1(a)). That is, Morakot initially moves westward to Taiwan, and then turns suddenly northward. It makes landfall around 1200 UTC 7 August. After it crosses the island at a slow movement speed, it moves northwestward to make a second landfall in the mainland China.

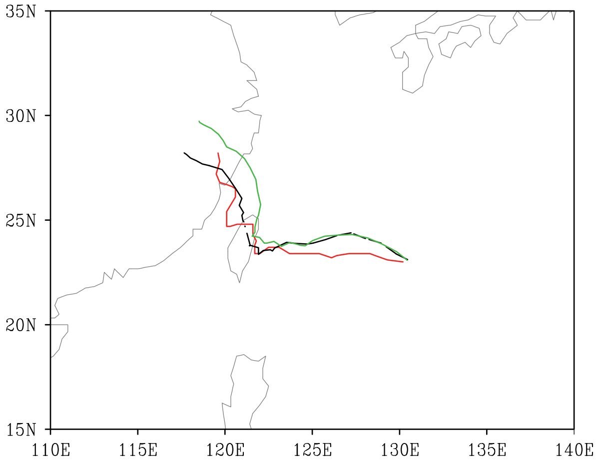

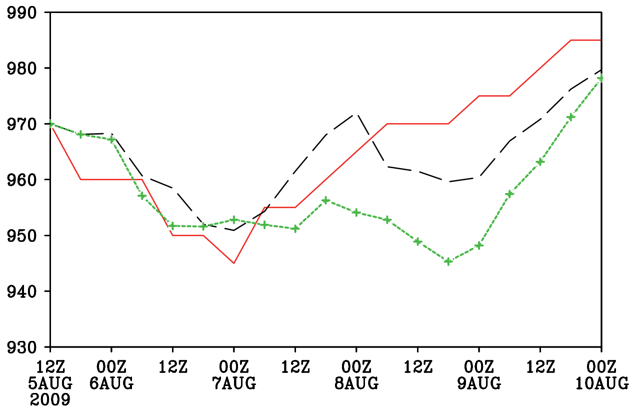

Figure 1. The observed and simulated TC tracks (a) and intensities (hPa; b). The red, black, and green line represents that from JMA best track, CTL, and TOP100 experiments, respectively.

The simulated track in TOP100 does not deviate much from that of CTL. It shows a similar initial westward and a sudden northward turning track, although it moves slightly faster and deflects further to the east. Given that the model configuration is the same as in CTL except that high topography over Taiwan Island is reduced, one can postulate that the sudden northward turning of Morakot is not caused by the terrain. It has been shown that the topography effect on the track is important when the scale of the topography is greater than the vortex R_{max} and the planetary beta parameter is less than the topographic beta parameter (Kuo *et al*., 2001). For the simulated Morakot, R_{max} exceeds 100 km, which is comparable to the terrain size. The large size is likely due to its formation from the monsoon gyre system, as the size of a mature TC is often determined by its initial disturbance (Rotunno and Emanuel, 1987). As a result, the effect of Taiwan orography on Morakot's track might be insignificant. As will be shown later, Morakot's northward track is primarily caused by the steering of a southwesterly monsoon surge.

Figure 1(b) compares the TC intensity between the simulations and the observation. In CTL, the TC intensifies sustainably until 7 August, and then weakens gradually while moving across Taiwan. Thereafter, it

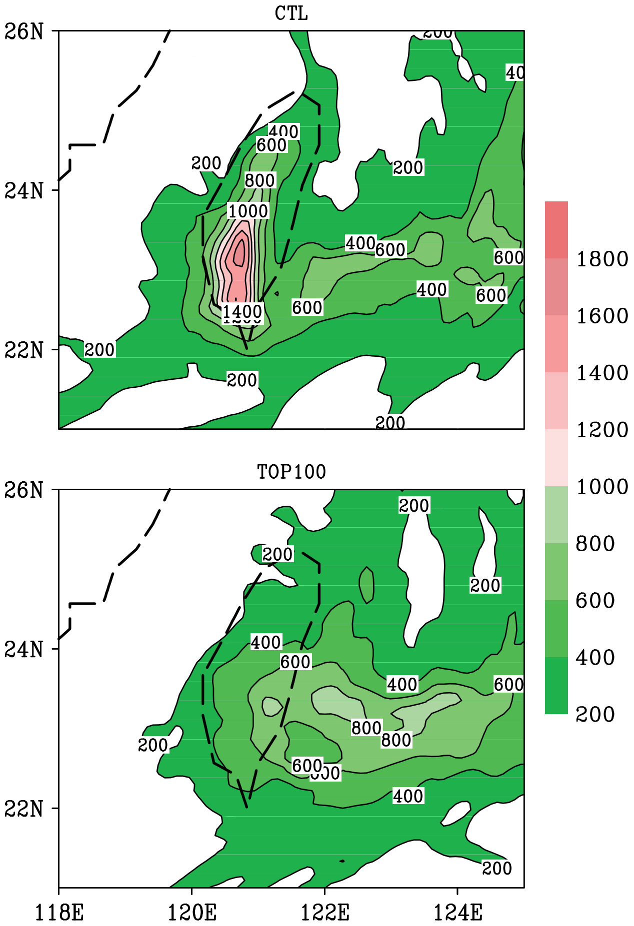

Figure 2. The model simulated accumulated rainfall amount during 108-h in CTL (a; unit: mm) and TOP100 (b).

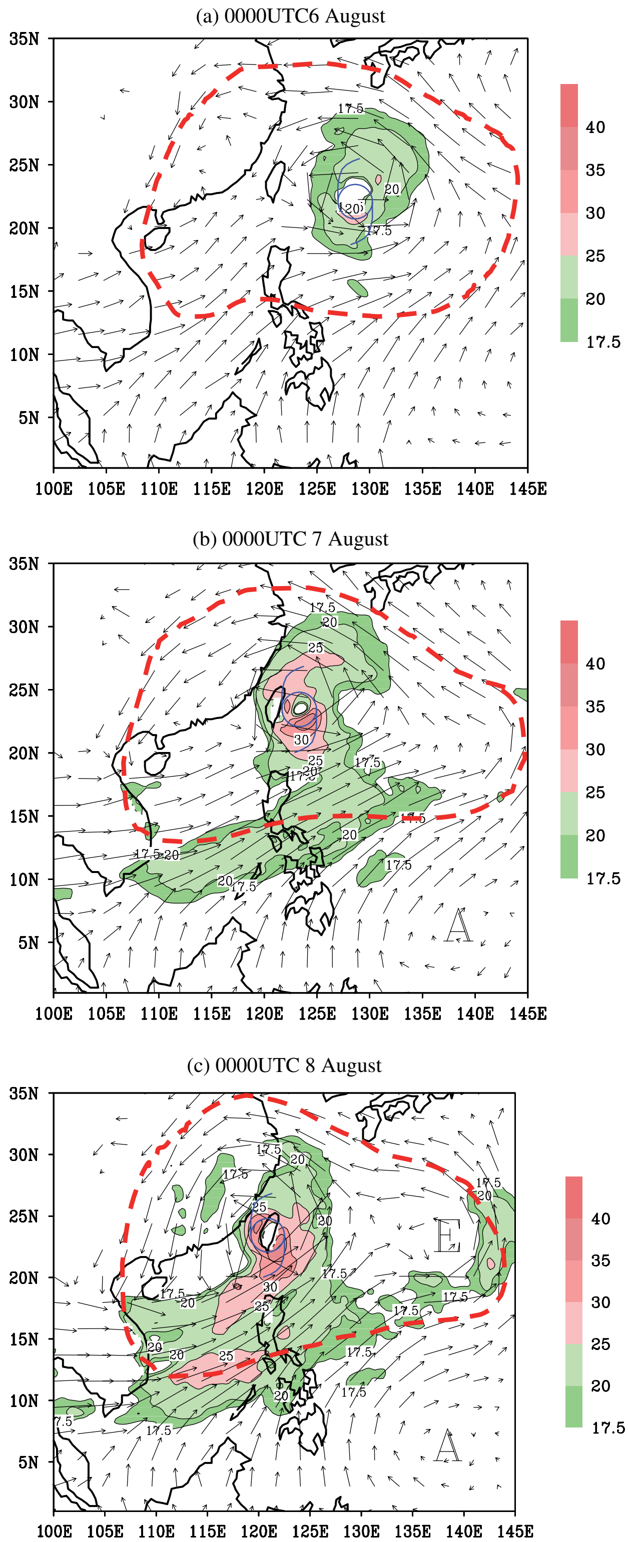

Figure 3. The low-level 950 hPa wind fields on 6 (a), 7 (b), and 8 August (c) in CTL. The shaded area indicates the wind velocity exceeds gale force 17.5 ms^{-1}. Hurricane symbol, *E* and *A* represent TC Morakot, TD Etau, and anticyclone associated with the dispersion of Morakot, respectively. The red dashed lines roughly outline the monsoon gyre.

re-intensifies slightly while entering the Taiwan Strait and weakens rapidly after the second landfall. The simulated intensity in CTL matches the observation reasonably well. As expected, the TC intensity in TOP100 is different from that in CTL. Prior to 7 August, the two simulations show similar evolution features. Thereafter, due to the reduction of Taiwan topography, the TC in TOP100 continues to intensify until 1800 UTC 8 August.

Figure 2 displays the accumulated rainfall amounts during the 108-h simulation period. In the CTL, the maximum accumulated rainfall is over 1800 mm and concentrates on Southern Taiwan. To better learn the temporal and spatial rainfall variation, we examine the 24-h accumulated rainfall on 8 August when TC Morakot just made landfall and moved over Taiwan. It is clear that the maximum rainfall concentrates on the southern of Island. This spatial rainfall distribution agrees with the observation (not shown) except that the simulated amount is somehow larger than the observed. In contrast, the simulated rainfall amount over Taiwan in TOP100 (Figure 2(b)) is much less. In fact, the rainfall maximum in TOP100 shifts to the east of Taiwan. The difference between CTL and TOP100 exceeds 1000 mm in Southern Taiwan, indicating the important role of the Taiwan topography in causing the extreme rainfall event.

As the terrain is always there, other factors must have roles in such a devastating event. Figure 3 shows the evolution of TC Morakot and its associated large-scale environmental flow in CTL. TC Morakot was indeed evolving within the monsoon gyre during the period of interest. That is, TC Morakot formed and was embedded in the huge monsoon gyre circulation. As it moves westward, there is a steady acceleration of the southwesterly monsoon flow to the south of Taiwan. For instance, on 6 August, the low-level 950 hPa gale force wind ($\geq$17.5 ms^{-1}) only exists near the core circulation of Morakot. Thereafter, an eastward overshooting of low-level southwesterly flow appeared along the southeastern periphery of the gyre. On 8 August, a strong monsoon surge that routinely exceeds gale force appears over the South China Sea.

Three mechanisms may be responsible for the enhanced southwesterly monsoon surge. First, it is simply attributed to an additive effect of the TC circulation and the monsoon southwesterly. As TC moves westward, the juxtaposition of the TC circulation and the monsoon gyre circulation enhances the wind speed to its southeastern periphery. It is found that the moisture flux and its convergence are greatly strengthened due to the juxtaposition of the monsoon gyre and TC (not shown). Second, the energy dispersion by both the monsoon gyre and TC may induce an anticyclonic circulation (denoted by 'A' in Figure 3) to its southeast side (Carr and Elsberry, 1995; Ge *et al.*, 2008), which may further enhance the monsoon surge flow through the enhanced pressure gradient. To demonstrate this process, an E-vector (Trenberth, 1986) is used to diagnose the energy propagation. It evidently shows a southeastward Rossby wave group velocity from the Typhoon Morakot (Figure 4). Although TC energy dispersion is often observed over the WNP, what is special about Morakot (2009) is that it had an unusually large eye and size. Furthermore, different from many typhoon cases characterized by an isolated vortex, Morakot was embedded in a large-scale monsoon gyre, which does not occur frequently (roughly once per years, see Lander, 1994). Based on previous observational and numerical studies (e.g. Carr and Elsberry, 1995; Ge *et al.*, 2008), the energy dispersion is sensitive to the vortex size. Thus, the

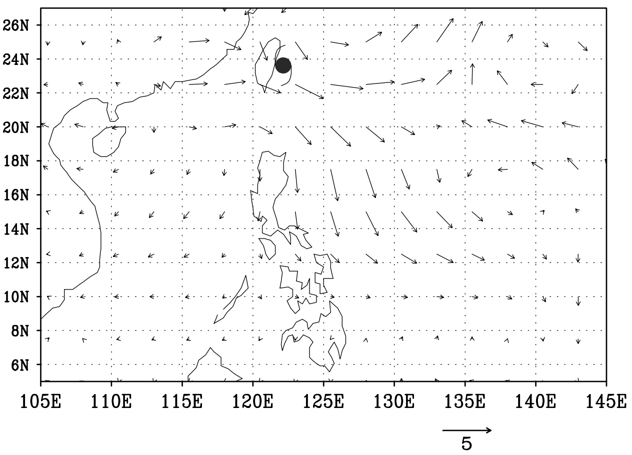

Figure 4. Horizontal map of E-vectors obtained by an 11-day period centered on 8 August. The hurricane symbol represents Typhoon Morakot.

combination of the unusually large Morakot and the large-scale monsoon gyre may greatly strengthen the energy dispersion.

The third mechanism is likely associated with the feedback from precipitation. The numerical results suggest that the interaction of the monsoon surge with Taiwan topography accounts for the extremely heavy rainfall in Taiwan. Therefore, it is likely a positive feedback between the heavy precipitation over Taiwan and the large-scale circulation. The heating associated with the heavy rainfall, on the one hand, may induce a Gill-type response, that is, a low-level southwesterly flow. The induced southwesterly, on the other hand, may further enhance the precipitation through the moisture transport. As the monsoon surge continues to accelerate, the region of strong winds wrap around the TC on 8 August (Figure 3(c)). The wind speed increases along the southeastern periphery of the TC, and a coma-shaped area of gale force wind is obvious. This asymmetric wind structure corresponds well to the spatial rainfall pattern. Although the TC center is located in Northern Taiwan, the strong persistent moisture supply by the southwesterly monsoon surge and its interaction with Taiwan orography favor the heavy rain in Southern Taiwan. The numerical simulation is consistent with satellite images of organized convective cloud bands to the south of TC (not shown).

The strengthened southwesterly monsoon surge brings excessive moisture into Taiwan. The uplift of the extremely large moisture flux by Taiwan CMR leads to the devastating rainfall over Southern island. The uplift effect can be clearly seen from the vertical velocity field. The maximum upward vertical velocity persists at the upslope side of the topography in Taiwan during 7 and 8 August. A comparison between CTL and TOP100 illustrates that a similar monsoon surge pattern is present in TOP100 (figure not shown). However, in the latter case with reduced topography, the large amount of the moisture is converged into the ocean region east of Taiwan, whereas much less rainfall appears in Southern Taiwan. Although the rainfall is very sensitive to the island topography, Morokot's track is not affected much by the topography. An interesting question is what causes its sudden northward track in both CTL and TOP100. By plotting the time–longitude cross section of the meridional wind along 20 °N (not shown), it clearly shows that the southerly wind increases rapidly at 0000 UTC 7 August, which is slightly prior to the timing of the northward turning. This relation suggests that the peripheral gale force wind to the southeast of TC Morakot acts as the steering flow to cause the TC track change. The monsoon surge induced sudden TC track change was discussed by Carr and Elsberry (1995). To confirm this monsoon surge track change mechanism, we also examine the evolution of the TC steering flow (averaged over 850–400 hPa) in TOP100. The evolution of the monsoon surge and the steering flow in TOP100 is very similar to that of CTL (not shown).

Thus, the sudden northward turning tracks in both CTL and TOP100 are ascribed to the steering effect of the large-scale monsoon surge.

4. Summary and discussion

In this study, the extremely heavy rainfall induced by TC Morakot (2009) is well simulated by a cloud-resolving model. After its formation in a monsoon gyre, Morakot moved westward and intensified into typhoon strength before making landfall on Taiwan. On 7 August, Morakot turned northward and moved slowly across Taiwan. During this period, it induced an extremely heavy rainfall in Southern Taiwan. In CTL, the model reasonably simulates the TC's motion and the spatial rainfall distribution. That is, the maximum rainfall is concentrated on the southern island, and the TC track shows a sudden northward turning. In a sensitivity experiment (TOP100) that reduces the topography over Taiwan, the maximum rainfall amount is greatly reduced over Taiwan, and the rainfall maximum is shifted to the ocean east of Taiwan. The TC track does not deviate much from that of CTL. The comparisons of CTL and TOP100 show that the extreme rainfall is mainly controlled by the presence of high topography due to its uplifting of a strong monsoon surge developed to the south of Taiwan.

The following three factors may contribute to the generation of the surge: the juxtaposition of the TC circulation and the monsoon gyre circulation, the Rossby wave energy dispersion by both the monsoon gyre and TC, and the feedback form the rainfall. The so-induced peripheral monsoon surge brings the excessive moisture into Taiwan region and leads to the extremely heavy rainfall through its interaction with Taiwan topography. Furthermore, it is likely a positive feedback between the diabatic heating and the circulation. Since the anomalous heating produced by the heavy rainfall may induce a Gill-type response, it will induce low-level westerly anomalies to the southwest as well. The monsoon surge also acts as the steering to drive the TC northward turning. The monsoon gyre-TC induced monsoon surge represents a local rainfall-flooding forecast challenge. By virtue of its persistence and organization, the monsoon southwesterly surge interacting with the orography may induce extremely heavy rainfall. In this study, we mainly focus on the evolution of large-scale circulation patterns. The detailed interaction among the typhoon, monsoon gyre, and topography requires further diagnoses. The relationship between the extreme rainfall and the TC large size and slow speed also deserves further careful examination.

Acknowledgements

The authors thank Drs Xiaqiong Zhou and Pang-Chi Hsu for valuable discussions. This work is supported by ONR Grants N000140710145 and N000140810256. X. Ge is also supported by NSF of China Grant 40875026. International Pacific Research Center is partially sponsored by the Japan Agency for Marine-Earth Science and Technology (JAMSTEC), NASA (NNX07AG53G), and NOAA (NA17RJ1230). This is SOEST contribution number 7875 and IPRC contribution number 650.

References

Carr LE, Elsberry LR. 1995. Monsoonal interactions leading to sudden tropical cyclone track changes. *Monthly Weather Review* **123**: 265–290.

Ge XY, Li T, Wang Y, Peng M. 2008. Tropical cyclone energy dispersion in a three-dimensional primitive equation model: upper tropospheric influence. *Journal of the Atmospheric Sciences* **65**: 2272–2289.

Hong SY, Dudhia J, Chen SH. 2004. A revised approach to ice-microphysical processes for the bulk parameterization of cloud and precipitation. *Monthly Weather Review* **132**: 103–120.

Kain JS, Fritch JM. 1993. Convective parameterization for mesoscale models: the Kain–Fritch scheme. The representation of cumulus convection in numerical models. *Meteorological Monographs American Meteor Society* **46**: 165–170.

Kuo HC, Williams RT, Chen JH, Chen YL. 2001. Topographic effects on barotropic vortex motion: no mean flow. *Journal of the Atmospheric Sciences* **58**: 1310–1327.

Kurihara Y, Bender MA, Tuleya RE, Ross RJ. 1995. Improvements in the GFDL hurricane prediction system. *Monthly Weather Review* **123**: 2791–2801.

Lander MA. 1994. Description of a monsoon gyre and its effect on the tropical cyclones in the western North Pacific during August 1991. *Weather Forecasting* **9**: 640–654.

Lonfat M, Marks FD, Chen SS Jr. 2004. Precipitation distribution in tropical cyclones using the Tropical Rainfall Measuring Mission (TRMM) microwave imager: a global perspective. *Monthly Weather Review* **132**: 1645–1660.

Noh Y, Cheon WG, Hong SY, Raasch S. 2003. Improvement of the K-profile model for the planetary boundary layer based on large eddy simulation data. *Boundary-Layer Meteorology* **107**: 401–427.

Peng MS, Chang SW. 2002. Numerical forecasting experiments on Typhoon Herb (1996). *Journal of the Meteorological Society of Japan* **80**: 1325–1338.

Trenberth KE. 1986. An assessment of the impact of transient eddies on the zonal flow during a blocking episode using localized Eliassen–Palm flux diagnostics. *Journal of the Atmospheric Sciences* **43**: 2070–2087.

Rotunno R, Emanuel KA. 1987. An air–sea interaction theory for tropical cyclones. Part II: evolutionary study using axisymmetric nonhydrostatic numerical model. *Journal of the Atmospheric Sciences* **44**: 542–561.

Wu CC, Kuo YH. 1999. Typhoons affecting Taiwan – Current understanding and future challenges. *Bulletin of the American Meteorological Society* **80**: 67–80.

Wu CC, Cheung KKW, Lo YY. 2009. Numerical study of the rainfall event due to interaction of Typhoon Babs (1998) and the Northeasterly Monsoon. *Monthly Weather Review* **137**: 2049–2064.

Yeh TC, Elsberry RL. 1993. Interaction of typhoons with the Taiwan orography. Part I: upstream track deflection. *Monthly Weather Review* **121**: 3193–3212.

